Biophysical Chemistry 151 (2010) 54–60

Contents lists available at ScienceDirect

Biophysical Chemistry

journal homepage: http://www.elsevier.com/locate/biophyschem

The effect of calcium binding on the unfolding barrier: A kinetic study on homologous α-amylases

Arpana Kumari [a,b,1], Tobias Rosenkranz [a,1], Arvind M. Kayastha [b,*], Jörg Fitter [a,*]

[a] Research Centre Jülich, ISB-2: Molecular Biophysics, D-52425 Jülich, Germany
[b] School of Biotechnology, Faculty of Science, Banaras Hindu University, Varanasi-221005, India

ARTICLE INFO

Article history:
Received 31 March 2010
Received in revised form 11 May 2010
Accepted 12 May 2010
Available online 19 May 2010

Keywords:
Alpha-amylase
Protein stability
Multi-domain protein
Calcium binding
Thermal unfolding
Eyring-plot

ABSTRACT

Extreme thermostabilities of proteins can be achieved by binding co-factors to the protein structures. For various α-amylases protein stabilization upon calcium binding is a well-known phenomenon. In the present study the mechanism of stabilization of three homologous α-amylases was investigated by measuring the unfolding kinetics with CD spectroscopy. For this purpose thermal unfolding kinetics of calcium saturated and calcium depleted enzymes were analyzed by means of Eyring-plots. The free energy change between the native and the transition state which characterized the unfolding barrier height was found to be proportional to the number of calcium ions bound to the protein structures. For the most thermostable α-amylases calcium binding caused a significant increase in the enthalpy change, which was partly compensated by increased entropy changes.

1. Introduction

In principle organisms can live under harsh conditions and in extreme environments. For example organisms are adapted to high temperatures, known as thermophiles (growth temperature 50–70 °C) or hyperthermophiles (growth temperatures >80 °C). Proteins from these organisms exhibit in general an uncommon thermal stability, although their folded structures are very similar to their mesophilic counterparts. As known from many studies performed in the last decades protein thermostability is achieved by a variety of strategies [1–5]. However, even mesophilic proteins can be extremely thermostable, and the task of elucidating determinants of thermostability is not confined to studies of proteins from extremophiles. In this respect the amylolytic enzyme α-amylase is a well-studied representative. α-Amylase catalyzes hydrolysis of α-1,4-glucosidic linkages of starch and has been isolated from various organisms (psychrophilic, mesophilic, thermophilic, and hyperthermophilic) showing an extremely broad range of melting temperatures (40–110 °C). This monomeric multi-domain protein (50–70 kDa) has become an important model system for the investigation of thermal adaptation of medium sized enzymes [6–9].

In order to elucidate the mechanisms of protein stabilization for α-amylases in more detail, at least two aspects are of particular importance. First, in most cases the unfolding transitions are irreversible, which is rather common for multi-domain proteins [10,11]. With the exception of α-amylase from *A. haloplanctis*, all known α-amylases exhibit an irreversible thermal unfolding transition, which is often accompanied by distinct aggregation of the unfolded state [8,12,13]. In some cases thermal unfolding transitions of α-amylases showed a partial reversibility by using high concentrations of co-solvents [11]. For unfolding induced by chemical denaturants at least some α-amylases show transitions with a high degree of reversibility [14–16]. As a consequence, due to the lacking reversibility of unfolding transitions, equilibrium thermodynamics is often not applicable. Therefore, kinetic measurements on the unfolding transition are of particular importance for comparative studies [13,17–20]. Using transition state theory, kinetic measurements can give valuable information about the thermodynamics of the unfolding barrier, which is related to the kinetic stability of a protein [21–23]. The second important aspect in protein stability is related to the fact that almost all known α-amylases contain at least one calcium ion per protein molecule [6,24]. As known from many previous studies, calcium binding in α-amylases can significantly increase protein stability. In most of these studies the melting temperatures (or to be more precise the apparent transition temperatures $T_{1/2}$) as well as the mid transition concentrations of urea or of GndHCl are significantly increased upon calcium binding [9,12,14,19,25,26]. In order to obtain more detailed insights on the impact of calcium binding

Abbreviations: BLA, *Bacillus licheniformis* α-amylase; TAKA, α-Amylase from *Aspergillus oryzae*; PPA, α-Amylase from pig pancreas; PGK, Phosphoglycerate kinase; GndHCl, Guanidine hydrochloride; EDTA, Ethylenediaminetetraacetic acid; Mops, 3-(N-morpholino)propanesulfonic acid; CD, Circular dicroism.

* Corresponding authors. Kayastha is to be contacted at Tel.: +91 542 2368331; fax: +91 542 2368693. Fitter, Tel.: +49 2461 612036; fax: +49 2461 612020.
E-mail addresses: kayasthabhu@gmail.com (A.M. Kayastha), j.fitter@fz-juelich.de (J. Fitter).

[1] Contributed equally to this work.

0301-4622/$ – see front matter © 2010 Elsevier B.V. All rights reserved.
doi:10.1016/j.bpc.2010.05.005

on the unfolding barrier we analyzed the unfolding kinetics of homologous α-amylases with different numbers of calcium binding sites in a comparative study. For this purpose we measured unfolding kinetics as a function of temperature in a calcium saturated and in a calcium depleted state with three different α-amylases, namely from *Bacillus licheniformis* (BLA) with three calcium binding sites, from *Aspergillus oryzae* (TAKA) with two calcium binding sites, and from pig pancreas (PPA) with one binding site (see Fig. 1). The effect of calcium binding on the unfolding barrier was analyzed in terms of thermodynamic parameters obtained by employing transition state theory.

2. Materials and methods

2.1. Enzymes

α-Amylase from *B. licheniformis* (BLA; purchased from Sigma) and from *A. oryzae* (TAKA; from Sigma) was obtained as lyophilized powder. Phosphoglycerate kinase from Bakers yeast (PGK; from Sigma) and α-amylase from pig pancreas (PPA, from Roche Applied Science) was obtained as ammonium sulfate precipitate. Powders were dissolved in buffer and all enzymes were desalted and transferred into desired buffers by the use of a desalting column (PD-10, Sephadex G-25, Amersham Biosciences). Unless stated otherwise a 10 mM Mops, 50 mM NaCl, 2 mM EDTA, pH 7.4 buffer was used for all proteins. Protein concentrations were determined by weight measurements of lyophilized protein and by measuring the absorption at 280 nm (PGK: ε_{280}: 20,340 $M^{-1}\,cm^{-1}$; TAKA: ε_{280}: 113,560 $M^{-1}\,cm^{-1}$; BLA: ε_{280}: 136,410 $M^{-1}\,cm^{-1}$; PPA: ε_{280}: 133,150 $M^{-1}\,cm^{-1}$).

2.2. Spectroscopic techniques and general procedures

Unfolding transitions were mainly monitored with CD spectroscopy. In some cases unfolding transitions were cross-checked in a fluorescence spectrometer, which was used to measure unfolding transitions (also partly at different protein concentrations) and to monitor protein aggregation during unfolding transitions.

2.3. CD spectroscopy

CD spectra in the far UV-region (200–280 nm) were recorded on a Jasco J-810 equipped with Peltier thermostated cuvette holder under constant nitrogen flow. For measurements characterizing the unfolding transitions as a function of temperature or of GndHCl concentrations the spectra were recorded in a 0.1 cm cell at protein concentration of 0.1–0.5 mg/ml, averaged over two scans using a scan rate of 50 nm/min. For kinetic studies a single spectrum was recorded with a scan rate of 100 nm/min. Finally all spectra measured with proteins were corrected for the buffer signal.

2.4. Fluorescence spectroscopy

Fluorescence emission spectra were recorded with protein solutions (protein concentration: 0.05–0.2 mg/mL) in quartz cuvettes (104F-QS, Hellma, Muehlheim, Germany) using a QuantaMaster spectrofluorimeter (QM-7) from Photon Technology International (Lawrenceville, NJ, USA). With excitation wavelengths of 280 nm for the α-amylases and of 295 nm for PGK we obtained emission spectra recorded between 300 and 450 nm. These spectra were corrected for background intensities as measured with pure buffer solutions. Unfolding transitions were analyzed by determining the wavelength of the emission intensity maximum (λ_{max}) as a function of environmental conditions (temperature, GndHCl). The detection and characterization of aggregates during unfolding transitions were performed by employing elastic light scattering with the same instrument. For this purpose we measured the elastic light scattering at 500 nm.

2.5. Kinetic studies and thermodynamic analysis

For kinetic studies all α-amylases were exposed to a calcium chelator (2 mM EDTA in the buffer) already 24 h before the measurements. As checked in previous studies, the applied procedure provides us with a homogenous population of calcium depleted α-amylase. The obtained enzymes remain folded and enzymatically active (at least for a few days) when stored at temperatures below 15 °C. In advance of time resolved measurements buffer solutions including respective concentrations of chemical denaturant were placed in the spectrometer for 5–10 min in order to reach thermal equilibrium at desired temperatures. After this a small amount of concentrated protein solution was rapidly added during permanent stirring and data acquisition was started. The dead time of this manual mixing procedure was about 20 s. The final protein concentration was between 2 and 10 μM. Typically we performed repetitive measurements every 60 s for a total time period of about 1 h. Unfolding transitions were monitored by taking the CD signal at 222 nm for samples at different temperatures or at different GndHCl concentrations as a function of time. For all data treatments and data presentations Origin7.5 (OriginLab Corp. Northhampton, MA, USA) was used. The time course of this signal was fitted with a mono-exponential decay

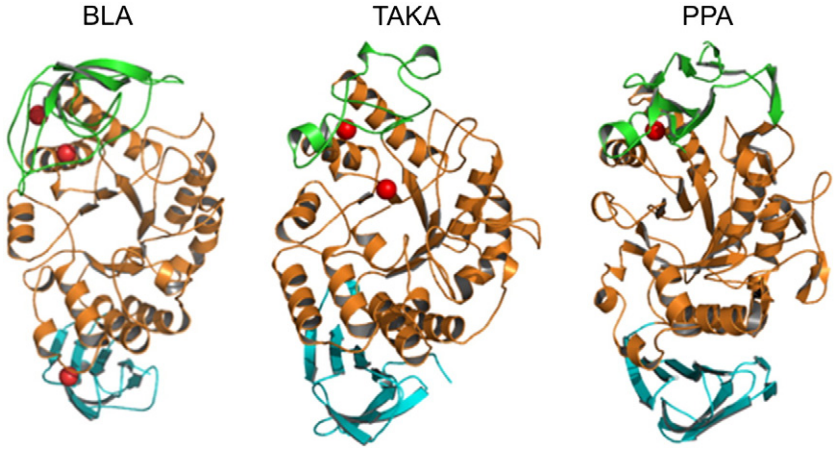

Fig. 1. Display of protein structures studied in this work (PDB code for BLA, 1BLI; for TAKA, 6TAA; for PPA, 1DHK). The color code represents the domain structure (green: domain B; orange domain A; cyan, domain C) while bound calcium ions are shown as red spheres. The conserved calcium (present in almost all α-amylases) is the only calcium ion bound in the PPA structure, while further bound calcium ions are present in TAKA (one additional calcium ion) and in BLA (two additional calcium ions). Structure presentations were produced using PyMOL (DeLano, W.L. The PyMOL Molecular Graphics System (2002), DeLano Scientific, San Carlos, CA, USA).

characterized by the unfolding rate constant K_u. According to the transition state theory the free energy change ΔG between the native state and the transitions state

$$\Delta G_F^{\#} = \Delta H_F^{\#} - T\Delta S_F^{\#} \quad (1)$$

which characterizes the unfolding barrier between the native and the unfolded state is related to the obtained unfolding rates K_u by the following relation [27]

$$K_u = k_o \cdot e^{-\Delta G_F^{\#}/RT}. \quad (2)$$

In this relation k_o, the so called pre-exponential factor, represents a largest possible rate constant for a specific chemical reaction in the absence of free energy barriers (see for example [23]). In order to obtain thermodynamic parameters from kinetic measurements as a function of temperature, unfolding rates were displayed in an Eyring-plot ($\ln(K_u/T)$ vs. $1/T$; see Fig. 3A) and the temperature dependence was analyzed using a linear fit ($y = -Ax + B$). From the slope of the linear fit we obtained ΔH and from the intercept with the y-axis we were able to determine ΔS. The dependence of K_u values on the concentration of GndHCl can be described by the following relation [28]:

$$K_u = K_{u,w} \cdot e^{m_u \cdot D}. \quad (3)$$

Here $K_{u,w}$ is the unfolding rate in buffer without GndHCl, D is the molar denaturant activity ($D = C_{0.5}[\text{GndHCl}]/(C_{0.5} + [\text{GndHCl}])$ with $C_{0.5} = 7.5$ M and the present denaturant concentration [GndHCl], see [29]), and the m_u value describes the sensitivity of changes in unfolding rates as a function of denaturant concentrations. The m_u values which are assumed to be proportional to changes in the accessible surface area (ASA) between the native and the transition state were obtained from Chevron-plots ($\ln(K_u)$ vs. D; see Fig. 3B).

3. Results and discussion

3.1. Kinetics for thermal and GndHCl induced unfolding

In an earlier study we measured unfolding kinetics of different α-amylases as a function of temperature with calcium saturated enzymes [13]. In order to complement our previous data we measured in the present study calcium depleted samples. In addition to calcium depleted α-amylases we investigated unfolding kinetics of another multi-domain protein which is not stabilized by a co-factor, namely the two-domain enzyme phosphoglycerate kinase (PGK) from Bakers yeast. As in our previous study we measured the unfolding kinetics by using CD spectroscopy. Typically kinetic measurements have been performed in a temperature range ±10–20 °C around the thermal transition temperature $T_{1/2}$ (as obtained with a heating rate 1 °C/min, see Table 1). The thermal transition temperature of calcium depleted α-amylases is strongly depending on the heating rate, similar to a behavior observed for calcium saturated enzymes [13]. As an example, for calcium depleted BLA the kinetic behavior of the CD signal is shown in Fig. 2A. In all cases the signal decay with time was well described by a single exponential decay within the limits of error (Fig. 2B). In a similar manner we measured unfolding kinetics for BLA, TAKA, and PGK at different GndHCl concentrations (PPA exhibits pronounced aggregation upon chemical denaturation which prevented quantitative analyses of the kinetics). For this purpose GndHCl concentrations around the mid transition concentrations $[\text{GndHCl}]_{1/2}$ were chosen. The latter were partly known from previous studies [11,25], but were measured again in the present work, also with different incubation times (1–24 h at 25 °C) of enzymes in the respective GndHCl concentrations (data not shown). In contrast to PGK and BLA which exhibit over the whole range of incubation times rather similar mid transition concentrations (for BLA with $[\text{GndHCl}]_{1/2} = 0.6$–$0.98$ M and for PGK with $[\text{GndHCl}]_{1/2} = 0.8$–$0.96$ M), TAKA shows a much stronger dependence of the mid transition concentration on the incubation time ($[\text{GndHCl}]_{1/2} = 0.34$–$3.7$ M). In all cases GndHCl induced unfolding kinetics exhibit mono-exponential decays under conditions used in the present study. Similar chemical denaturant induced single phase unfolding transitions with rather slow kinetics were observed in previous studies [15,30]. However, in a recent study on α-amylase from mung beans transitions with two phases were observed at high GndHCl concentrations (fast transitions measured with stop-flow mixing). Much slower transitions with a single phase appeared at low GndHCl concentrations [20].

For calcium saturated samples [13] and for PGK unfolding rates as obtained from fits with a mono-exponential decay exhibited an error of ±5–7% and for calcium depleted samples an of error of ±7–15% was observed. In some cases thermal as well as chemical unfolding kinetics was measured by employing tryptophan fluorescence which gave results with the same unfolding rates within the limits of error (data not shown). This cross-check indicates that the observed unfolding transition appears rather cooperative, with the disintegration of tertiary and secondary structure elements taking place simultaneously, see also [9,30]. Furthermore, in the case of heat induced unfolding often aggregation of unfolded states was observed. Similar to observations with calcium saturated samples aggregation of calcium depleted enzymes takes place only after the unfolding transition [13].

3.2. Thermodynamic characterization of the unfolding transition and the impact of calcium on the unfolding barrier

The obtained unfolding rates K_u are presented in an Eyring-plot for thermal unfolding (Fig. 3A) and in a Half–Chevron-plot for denaturant induced unfolding (Fig. 3B). By employing simple linear regression fits to the experimental data the relevant thermodynamic parameters were determined as listed in Table 1. The most obvious feature of our

Table 1
Thermodynamic parameter of the unfolding transition obtained from Eyring-plots.

	$T_{1/2}$[a] [°C]	ΔH [kJ/mol]	ΔS [J/mol/K]	$\Delta H/RT_{25}$	$\Delta S/R$	$\Delta G/RT_{25}$	K_u at T_{25}[b] [s^{-1}]	$K_{u,w}$ at T_{25}[c] [s^{-1}]	m_u [M^{-1}]
PPA_ca[d]	65	204.73	506.26	82.63	60.89	21.74	$1.09 \cdot 10^{-07}$	n.d.	n.d.
TAKA_ca[d]	71	315.03	820.46	127.15	98.68	28.47	$1.30 \cdot 10^{-10}$	n.d.	n.d.
BLA_ca[d]	102	360.56	856.97	145.52	103.07	42.45	$1.10 \cdot 10^{-16}$	n.d.	n.d.
PGK	62	473.27	1355.83	191.01	163.07	27.94	$2.20 \cdot 10^{-10}$	$8.07 \cdot 10^{-10}$	24.63
PPA_noca	48	286.24	804.17	115.53	96.72	18.81	$2.02 \cdot 10^{-06}$	n.d.	n.d.
TAKA_noca	57	109.48	234.38	44.19	28.19	16.00	$3.38 \cdot 10^{-05}$	$9.86 \cdot 10^{-06}$	1.59
BLA_noca	52	143.13	339.06	57.77	40.78	16.99	$1.26 \cdot 10^{-05}$	$4.07 \cdot 10^{-05}$	4.59

$T_{25} = 25$ °C (298 K), $R \cdot T_{25} = 2.47$ kJ/mol with $R = 8.3144$ J/mol/K.
ΔH, ΔS, and m_u values as obtained from fits are characterized by the following errors: For calcium saturated samples the error in ΔH and ΔS was ±4–6%, for calcium depleted samples and for PGK the error in ΔH and ΔS was ±15–20% and in m_u ±4–8%.
[a] Transition temperatures were measured with heating rates of 1 °C/min, taken from [13].
[b] Unfolding rates obtained from extrapolations to room temperatures ($T = 25$ °C) of data shown in the Eyring-plot (Fig. 3A).
[c] Unfolding rates obtained from extrapolations to GndHCl concentration of 0 M (Fig. 3B).
[d] Experimental data were taken from a previous work [13].

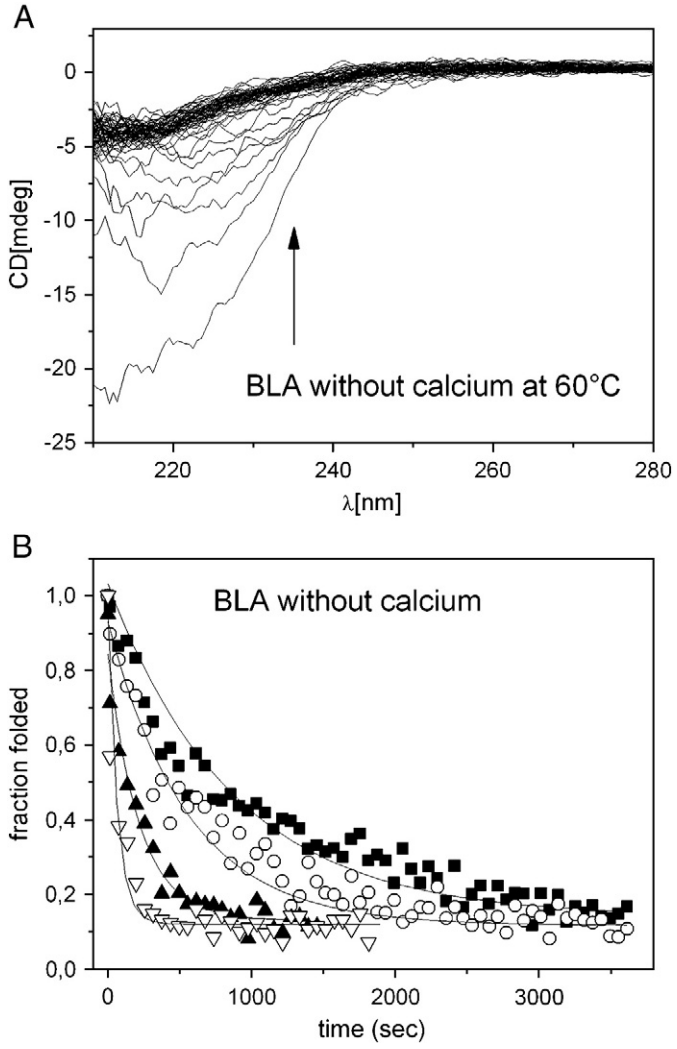

Fig. 2. (A) CD spectra of calcium depleted BLA at 60 °C are shown as function of time for a time period of 1 h measured every 60 s. The arrow indicates the chronology of measured spectra (from earliest to later measurements). (B) The kinetic behavior was analyzed by plotting the CD signal at 222 nm as measured with different temperatures as a function of time. Data are shown for the following temperatures (from slowest to fastest transitions): 47 (solid squares), 51 (open circles), 60 (solid triangles), 65 (open triangles) °C. In order to obtain the fraction of folded protein as a function of time we used reference measurements for a native and a fully unfolded sample, measured with the same protein concentration either in native buffer at 25 °C or in 6 M GndHCl, respectively.

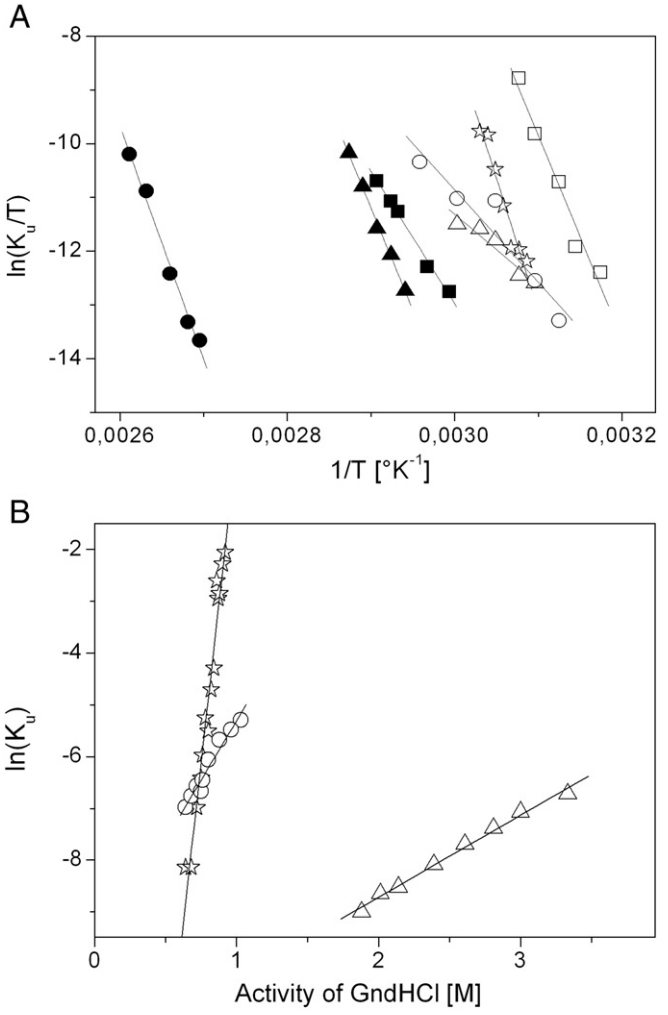

Fig. 3. (A) Eyring-plots with the temperature dependence of unfolding rates are shown for PGK (stars) and for α-amylases in a calcium depleted state (open symbols) and in the calcium saturated state (solid symbols): PPA (squares), TAKA (triangles), and BLA (circles). Related thermodynamic parameters as obtained from linear fits (solid lines) are given in Table 1. (B) Half–Chevron plots are shown for PGK (stars), for BLA (circles), and for TAKA (triangles), the latter for calcium depleted samples.

analysis is given by the fact that the free energy changes $\Delta G_F^{\#}$ between the native state and the transition state are more or less proportional to the transition temperatures (Fig. 4). This indicates that kinetic stability has a major impact on the thermostability of our proteins. It has already been shown in various previous studies that extremely slow unfolding rates are a key feature in achieving a pronounced thermostability [31–34]. Furthermore the data indicates that thermostability is related to the "extent" of calcium binding. For calcium depleted α-amylases the transition temperatures vary around 50 °C, but do not differ significantly between homologous α-amylases. This feature is also visible by rather similar free energy change values ($\Delta G_F^{\#}/RT \sim 17 \pm 2$) for the corresponding enzymes (see Table 1). In contrast to this, for calcium saturated α-amylases transition temperatures as well as free energy changes differ significantly. A larger number of calcium binding sites (i.e. number of bound calcium ions per enzyme molecule under calcium saturation conditions) are related to an increasing free energy change. The difference of free energy changes between those obtained from calcium depleted

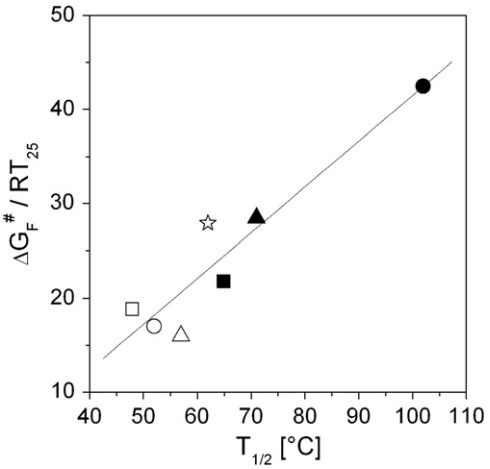

Fig. 4. The free energy change $\Delta G_F^{\#}$ (normalized to RT at room temperature) is plotted against the corresponding transition temperature as measured with a heating rate of 1 °C/min. Despite a certain scatter of the presented data, the proportionality between both parameters is visible, at least qualitatively (for the legend see Fig. 3).

samples and from calcium saturated samples increases with the number of bound calcium ions in the respective enzymes (PPA with $\Delta\Delta G^{\#}_F/RT = 2.9$, TAKA with $\Delta\Delta G^{\#}{}_F/RT = 12.47$ and BLA with $\Delta\Delta G^{\#}{}_F/RT = 25.46$). It is known that all class-13 α-amylases share a common (conserved) calcium binding site, which is located in the interface between domain A and domain B in close proximity to the active site (see Fig. 1). Only this calcium is present in the PPA structure. In addition and in close proximity to the conserved calcium binding site, many homologues have a second metal binding site, where in TAKA and in BLA a second calcium ion is bound. In the case of BLA these two calcium ions form a triade together with a Na^+ ion. Furthermore, BLA exhibits a third metal binding site at the interface between domain A and domain C (see BLA structure in Fig. 1) [35]. In particular for other very thermostable homologous such a third binding site was observed (e.g., α-amylases from *B. amyloliquefaciens* or from *P. woesi* [36,37]). Since this third latter binding site is located at strategically important position in the protein structure, it may strengthen the interaction between domain A and C and thereby explain the extreme high transition temperatures of these enzymes. In addition to the absolute number of bound ions also the extent and the geometry of coordination of the ligand is important for protein stability (see for example the triade in BLA), because the latter is related to the strength of the ligand binding [38]. Although the ΔG values as obtained from the set of α-amylases analyzed in the present work exhibit a striking proportionality to the number of bound calcium ions in the respective proteins structures, we cannot rule out that other factors than the number of bound calcium ions play an important or even a dominating role (e.g., Ca–Na–Ca triade in BLA).

One advantage to measure and to analyze unfolding rate constants is related to the fact that changes in enthalpy and in entropy between the native state and the transition state can be deduced from Eyring-plots (Table 1). Although a straight forward interpretation of enthalpy and entropy changes is difficult, mainly because it is *a priori* not possible to distinguish between contribution from the protein and that from the solvent, a few interesting results obtained from our analysis are worth to be discussed in detail.

(1) With respect to smaller single-domain proteins we obtained rather large absolute values for enthalpy changes as well as for entropy changes for our proteins. This was not unexpected for the multi-domain proteins studied here, since the increase of changes in enthalpy and entropy generally increases with the length of the polypeptide chain. However, due to the general phenomenon of enthalpy–entropy compensation the corresponding free energy changes are not necessarily larger for the investigated multi-domain proteins as compared to smaller (single-domain) thermostable proteins [21,22,38–40].

(2) The stabilization upon calcium binding in terms of thermodynamic parameters is similar for TAKA and BLA, but rather different for PPA. Calcium depleted BLA and TAKA exhibit ΔH and ΔS values which are drastically reduced by a similar degree (~30–40%) for both α-amylases as compared to calcium saturated samples. As a consequence smaller absolute ΔG values are observed for calcium depleted samples, consistent with the lower thermal stability (see also transition temperatures in Table 1). The major contribution to protein stabilization upon calcium binding is caused by large positive enthalpy change, which is counter balanced to a considerable extent by an accompanied increase of ΔS. A possible explanation for this behavior is may be given by the fact that in contrast to the native state, the transition state has already released the bound calcium and exhibits a much larger conformational flexibility as compared to the native state. For PPA the results are quite different. Here the absolute values for ΔH and ΔS are larger for calcium depleted samples as compared to calcium saturated samples. Due to the fact that the entropy change for calcium depleted PPA increases stronger than the enthalpy change (upon calcium depletion) the calcium depleted PPA is slightly less thermostable as compared to calcium saturated PPA. Recently, for α-amylase from *Bacillus halmapalus* (BHA) a change in activation energies E_a (proportional to ΔH) during denaturation was found to be 101 kJ/mol for the calcium depleted sample and 123 kJ/mol for the calcium saturated enzyme [41]. Compared to our data the stabilization mechanisms related to calcium binding in BHA (which is assumed to have three calcium binding sites [26]) are similar to that of TAKA and BLA, but exhibited a much smaller increase of ΔH upon calcium binding.

(3) Another important question is related to the extent to which the native state differs from the transition state, structurally and with respect to solvent interaction. While for BLA and TAKA calcium binding seems to have a strong influence on the entropy and enthalpy changes between native and transition state for PPA the entropy change is most probable not strongly related to calcium binding. We observe only 30–35% larger entropy changes for calcium depleted samples as compared to calcium saturated samples. In contrast BLA and TAKA exhibit a two- to threefold larger entropy and enthalpy changes for calcium saturated samples as compared to calcium depleted samples. For BLA and TAKA this may indicate that in the case of calcium binding the transition state is characterized by a higher polypeptide chain flexibility, a less compact protein structure, and (or) more pronounced solvent interactions as compared to the native state. Then a large positive ΔH reflects the loss of interactions in the transition state that are present in the native state (most probably also including calcium binding interactions). Breaking these interactions seems to result in a less ordered transition state and an increased entropy of the system [21]. If we compare only enzymes without co-factors bound to the protein structure (including PGK) a significant difference for BLA and TAKA on the one hand, and for PPA and PGK on the other hand is visible. The latter do show enthalpy changes and in particular entropy changes which are larger as compared to BLA and TAKA. As already mentioned above huge positive ΔS values indicate less ordered transition state structures as compared to the native state. At least for PGK this is supported by a remarkable large positive m_u value. This value indicates a much stronger denaturant interaction, corresponding to a bigger solvent exposed protein surface and to a less ordered protein structure of the transition state as compared to the native state. Consequently, for BLA and even more for TAKA a much smaller m_u value is accompanied by a much smaller entropy change. Such a large m_u value (~24 M^{-1}) as obtained for the investigated PGK is remarkable. Typically these values are much smaller (in particular for smaller proteins ~0.1–2 M^{-1}) [39]. However, at least for phosphoglycerate kinases big m_u values seem to be a common feature. A study employing tryptophan fluorescence (monitoring only the C-terminal domain) exhibits a m_u value in the order of 12 M^{-1} for a homologous PGK from *B. stearothermophilus* [42].

(4) Extrapolated unfolding rates for room temperatures (25 °C) were obtained from Eyring-plots and from Half–Chevron plots (Table 1). Taking into account the errors in the linear regression fitting which are significantly enhanced by extrapolations, at room temperatures the errors in K_u are relatively large. Despite of this error, values obtained with both methods are at least in the same order of magnitude, ranging from 10^{-5} s^{-1} for enzymes with transition temperatures around 50 °C to 10^{-16} s^{-1} for calcium saturated BLA with $T_{1/2}$ of 102 °C. Compared to our result for PGK with K_u ~2.2–8.0•10^{-10} s^{-1} the homologous analog from *B. stearothermophilus* showed a very similar rate (K_u ~7.6•10^{-10} s^{-1}) [42]. In addition to extrapolations from Eyring- or Half–Chevron plots the room

temperature unfolding rate constant can be calculated directly by using Eq. (2) (see section Materials and methods). For this purpose the pre-exponential factor has to be known. In the original Erying theory this factor is given by:

$$k_0 = \kappa \frac{k_B T}{h} \approx 6 \cdot 10^{12} s^{-1} \text{ at } 25\ ^\circ C.$$

Here κ is the transmission factor (typically assumed to be 1), k_B is the Boltzmann constant, h is the Planck constant, and T is the temperature. In contrast to assumptions made in the Eyring theory, protein folding/unfolding transitions involve formation and breakage of many weak intramolecular interactions rather than a formation or cleavage of a single covalent bond. Therefore the above given pre-exponential factor will not be useful for our analysis. For protein folding/unfolding reactions segmental diffusion processes of polypeptide chain fragments will determine the rate limitation. In principle this factor can be quite different for individual proteins. Most probably it will also depend on the polypeptide chain length (i.e. on the proteins size). For smaller single-domain proteins pre-exponential factors in the order of 10^5–10^8 have been assumed [23,43]. The multi-domain proteins investigated in this study are characterized by a polypeptide chain length of about 450–500 residues. Applying Eq. (2) we received the best agreement with K_u values obtained from the Eyring-plot fittings by using a pre-exponential factor of $3 \cdot 10^2$ (3.3 ms). Although a comparison with values from the literature is not straightforward (typically in these studies folding rates with small single-domain proteins with an averaged length of 80 residues characterized by a two-state folding process taking place within 10 μs were measured from urea or GndHCl unfolded proteins [43]), we observe significantly slower transitions with much smaller pre-exponential factors for multi-domain protein unfolding transitions as compared to what has been observed in published studies. However, to our knowledge pre-exponential factors have not yet been determined for multi-domain proteins. Further studies, in particular on folding transitions, with multi-domain proteins should give an indication whether relatively small pre-exponential factors (slow transition processes) are representative for larger multi-domain proteins which are generally characterized by multi-state transitions.

4. Conclusion

In the present study we demonstrated that the analysis of temperature dependent unfolding kinetics is a powerful method to obtain detailed insights about characteristics of the unfolding barrier which is a key feature of the thermostability for many enzymes. In the case of homologous α-amylases the presented data indicate that beside a conserved calcium ion which is present in almost all α-amylases, the existence of one or two additional calcium ions as bound to more thermostable enzymes drastically increases the free energy of the unfolding barrier. This increase as observed for calcium saturated with respect to calcium depleted enzymes is proportional to the number of bound calcium ions and is generated by enthalpic contributions, which is partly compensated by increased entropy changes. Although further properties of homologous α-amylases may also contribute significantly to the individual thermostability of the respective enzyme (see for example a comparison of BLA and BAA [9,30]), extreme thermostabilities of α-amylases with melting temperatures above 80 °C are only achieved by using calcium (ligand) binding. In this regard the presented study offers a valuable attempt to rationalize the thermodynamic basis of calcium stabilization in α-amylases.

Acknowledgements

AK would like to thank DAAD (Sandwich Model Fellowship) for funding to carry out this work in Germany. TR acknowledges financial support by the International Helmholtz Research School on Biophysics and Soft Matter ("BioSoft"). JF thanks Prof. G. Büldt for sustainable and continuous support in his institute.

References

[1] K.O. Stetter, Extremophiles and their adaptation to hot environments, FEBS Lett. 452 (1999) 22–25.
[2] R. Jaenicke, G. Bohm, The stability of proteins in extreme environments, Curr. Opin. Struct. Biol. 8 (1998) 738–748.
[3] C. Vieille, G.J. Zeikus, Hyperthermophilic enzymes: sources, uses, and molecular mechanisms for thermostability, Microbiol. Mol. Biol. Rev. 65 (2001) 1–43.
[4] G.A. Petsko, Structural basis of thermostability in hyperthermophilic proteins, or "there's more than one way to skin a cat", Methods Enzymol. 334 (2001) 469–478.
[5] K.A. Luke, C.L. Higgins, P. Wittung-Stafshede, Thermodynamic stability and folding of proteins from hyperthermophilic organisms, FEBS J. 274 (2007) 4023–4033.
[6] M. Vihinen, P. Mantsala, Microbial amylolytic enzymes, Crit Rev. Biochem. Mol. Biol. 24 (1989) 329–418.
[7] B. Svensson, Protein engineering in the alpha-amylase family — catalytic mechanism, substrate-specificity, and stability, Plant Mol. Biol. 25 (1994) 141–157.
[8] J.E. Nielsen, T.V. Borchert, Protein engineering of bacterial alpha-amylases, Biochim. Biophys. Acta 1543 (2000) 253–274.
[9] J. Fitter, Structural and dynamical features contributing to thermostability in alpha-amylases, Cell Mol. Life Sci. 62 (2005) 1925–1937.
[10] H. Lilie, R. Seckler, Folding and association of multi-domain and oligomeric proteins, in: J. Buchner, T. Kiefhaber (Eds.), Protein Folding Handbook, Wiley-VCH Verlag, Weinheim, Germany, 2005, pp. 32–72.
[11] K.H. Strucksberg, T. Rosenkranz, J. Fitter, Reversible and irreversible unfolding of multi-domain proteins, Biochim. Biophys. Acta 1774 (2007) 1591–1603.
[12] G. Feller, D. d'Amico, C. Gerday, Thermodynamic stability of a cold-active alpha-amylase from the Antarctic bacterium *Alteromonas haloplanctis*, Biochemistry 38 (1999) 4613–4619.
[13] C. Duy, J. Fitter, Thermostability of irreversible unfolding alpha-amylases analyzed by unfolding kinetics, J. Biol. Chem. 280 (2005) 37360–37365.
[14] H. Fukada, K. Takahashi, J.M. Sturtevant, Differential scanning calorimetric study of the thermal unfolding of Taka-amylase A from *Aspergillus oryzae*, Biochemistry 26 (1987) 4063–4068.
[15] A.R. Nazmi, T. Remisch, H.J. Hinz, Ca-binding to *Bacillus licheniformis* alpha-amylase (BLA), Arch. Biochem. Biophys. 453 (2006) 18–25.
[16] R.S. Sai Kumar, S.A. Singh, A.G. Rao, Conformational stability of alpha-amylase from malted sorghum (*Sorghum bicolor*): reversible unfolding by denaturants, Biochimie 91 (2009) 548–557.
[17] S.J. Tomazic, A.M. Klibanov, Mechanisms of irreversible thermal inactivation of *Bacillus* alpha-amylases, J. Biol. Chem. 263 (1988) 3086–3091.
[18] M. Violet, J.C. Meunier, Kinetic study of the irreversible thermal denaturation of *Bacillus licheniformis* alpha-amylase, Biochem. J. 263 (1989) 665–670.
[19] A. Tanaka, E. Hoshino, Calcium-binding parameter of *Bacillus amyloliquefaciens* alpha-amylase determined by inactivation kinetics, Biochem. J. 364 (2002) 635–639.
[20] P. Tripathi, H. Hofmann, A.M. Kayastha, R. Ulbrich-Hofmann, Conformational stability and integrity of alpha-amylase from mung beans: evidence of kinetic intermediate in GdmCl-induced unfolding, Biophys. Chem. 137 (2008) 95–99.
[21] S.E. Jackson, A.R. Fersht, Folding of chymotrypsin inhibitor 2. 2. Influence of proline isomerization on the folding kinetics and thermodynamic characterization of the transition state of folding, Biochemistry 30 (1991) 10436–10443.
[22] S. Cavagnero, Z.H. Zhou, M.W. Adams, S.I. Chan, Unfolding mechanism of rubredoxin from *Pyrococcus furiosus*, Biochemistry 37 (1998) 3377–3385.
[23] A. Bachmann, T. Kiefhaber, Kinetic mechanisms in protein folding, in: J. Buchner, T. Kiefhaber (Eds.), Protein Folding Handbook, vol. 1, Wiley-VCH Verlag, Weinheim, Germany, 2005, pp. 379–410.
[24] B.L. Vallee, E.A. Stein, W.N. Sumerwell, E.H. Fischer, Metal content of alpha-amylases of various origins, J. Biol. Chem. 234 (1959) 2901–2905.
[25] J. Fitter, R. Herrmann, N.A. Dencher, A. Blume, T. Hauss, Activity and stability of a thermostable alpha-amylase compared to its mesophilic homologue: mechanisms of thermal adaptation, Biochemistry 40 (2001) 10723–10731.
[26] A.D. Nielsen, M.L. Pusey, C.C. Fuglsang, P. Westh, A proposed mechanism for the thermal denaturation of a recombinant *Bacillus halmapalus* alpha-amylase—the effect of calcium ions, Biochim. Biophys. Acta 1652 (2003) 52–63.
[27] H. Eyring, The activated complex in chemical reactions, J. Chem. Phys. 3 (1935) 107–115.
[28] A. Ikai, W.W. Fish, C. Tanford, Kinetics of unfolding and refolding of proteins. II. Results for cytochrome c, J. Mol. Biol. 73 (1973) 165–184.
[29] M.J. Parker, J. Spencer, A.R. Clarke, An integrated kinetic analysis of intermediates and transition states in protein folding reactions, J. Mol. Biol. 253 (1995) 771–786.
[30] J. Fitter, S. Haber-Pohlmeier, Structural stability and unfolding properties of thermostable bacterial alpha-amylases: a comparative study of homologous enzymes, Biochemistry 43 (2004) 9589–9599.
[31] S. Cavagnero, D.A. Debe, Z.H. Zhou, M.W. Adams, S.I. Chan, Kinetic role of electrostatic interactions in the unfolding of hyperthermophilic and mesophilic rubredoxins, Biochemistry 37 (1998) 3369–3376.
[32] K. Ogasahara, M. Nakamura, S. Nakura, S. Tsunasawa, I. Kato, T. Yoshimoto, K. Yutani, The unusually slow unfolding rate causes the high stability of pyrrolidone carboxyl peptidase from a hyperthermophile, *Pyrococcus furiosus*: equilibrium and kinetic studies of guanidine hydrochloride-induced unfolding and refolding, Biochemistry 37 (1998) 17537–17544.

[33] T. Collins, M.A. Meuwis, C. Gerday, G. Feller, Activity, stability and flexibility in glycosidases adapted to extreme thermal environments, J. Mol. Biol. 328 (2003) 419–428.
[34] R. Sterner, W. Liebl, Thermophilic adaptation of proteins, Crit Rev. Biochem. Mol. Biol. 36 (2001) 39–106.
[35] M. Machius, N. Declerck, R. Huber, G. Wiegand, Activation of *Bacillus licheniformis* alpha-amylase through a disorder→ order transition of the substrate-binding site mediated by a calcium—sodium—calcium metal triad, Structure 6 (1998) 281–292.
[36] A.M. Brzozowski, D.M. Lawson, J.P. Turkenburg, H. Bisgaard-Frantzen, A. Svendsen, T.V. Borchert, Z. Dauter, K.S. Wilson, G.J. Davies, Structural analysis of a chimeric bacterial alpha-amylase. High-resolution analysis of native and ligand complexes, Biochemistry 39 (2000) 9099–9107.
[37] A. Linden, O. Mayans, W. Meyer-Klaucke, G. Antranikian, M. Wilmanns, Differential regulation of a hyperthermophilic alpha-amylase with a novel (Ca, Zn) two-metal center by zinc, J. Biol. Chem. 278 (2003) 9875–9884.
[38] A. Loaiza, K.M. Armstrong, B.M. Baker, M.M. Abu-Omar, Kinetics of thermal unfolding of phenylalanine hydroxylase variants containing different metal cofactors (Fe-II, Co-II, and Zn-II) and their lsokinetic relationship, Inorg. Chem. 47 (2008) 4877–4883.
[39] S.E. Jackson, How do small single-domain proteins fold? Fold Des. 3 (1998) R81–R91.
[40] B.J. Henriques, L.M. Saraiva, C.M. Gomes, Probing the mechanism of rubredoxin thermal unfolding in the absence of salt bridges by temperature jump experiments, Biochem. Biophys. Res. Commun. 333 (2005) 839–844.
[41] A.D. Nielsen, C.C. Fuglsang, P. Westh, Effect of calcium ions on the irreversible denaturation of a recombinant *Bacillus halmapalus* alpha-amylase: a calorimetric investigation, Biochem. J. 373 (2003) 337–343.
[42] M.J. Parker, R.B. Sessions, I.G. Badcoe, A.R. Clarke, The development of tertiary interactions during the folding of a large protein, Fold Des 1 (1996) 145–156.
[43] J. Kubelka, J. Hofrichter, W.A. Eaton, The protein folding 'speed limit', Curr. Opin. Struct. Biol. 14 (2004) 76–88.